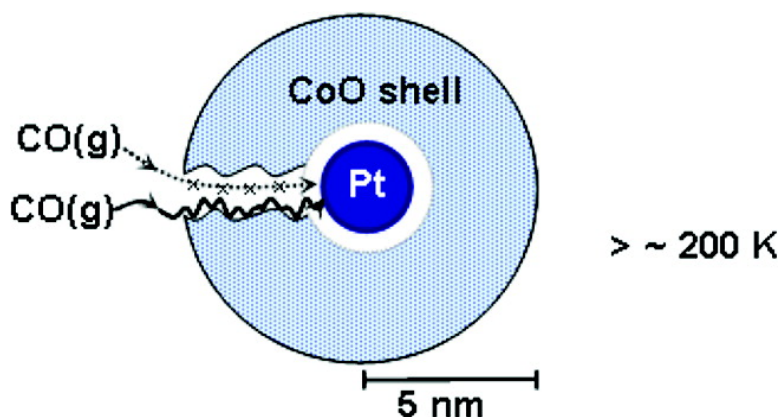


IR Spectroscopic Observation of Molecular Transport through Pt@CoO Yolk–Shell Nanostructures

Sunhee Kim, Yadong Yin, A. Paul Alivisatos, Gabor A. Somorjai, and John T. Yates

J. Am. Chem. Soc., **2007**, 129 (30), 9510-9513 • DOI: 10.1021/ja072588g • Publication Date (Web): 06 July 2007

Downloaded from <http://pubs.acs.org> on February 16, 2009



More About This Article

Additional resources and features associated with this article are available within the HTML version:

- Supporting Information
- Links to the 3 articles that cite this article, as of the time of this article download
- Access to high resolution figures
- Links to articles and content related to this article
- Copyright permission to reproduce figures and/or text from this article

[View the Full Text HTML](#)



ACS Publications
 High quality. High impact.

IR Spectroscopic Observation of Molecular Transport through Pt@CoO Yolk–Shell Nanostructures

Sunhee Kim,[†] Yadong Yin,[‡] A. Paul Alivisatos,[§] Gabor A. Somorjai,[§] and John T. Yates, Jr.^{*,†}

Contribution from the Surface Science Center, Department of Chemistry, University of Pittsburgh, Pittsburgh, PA 15260, Department of Chemistry, University of California, Riverside, CA 92521, and Department of Chemistry, University of California, Berkeley, CA 94720

Received April 13, 2007; E-mail: johnt@virginia.edu

Abstract: FTIR spectroscopy has been used to monitor the transport of CO to the Pt cores of Pt@CoO nanoparticles forming CO/Pt species. It was found that external Pt sites are not present on the outer surfaces of the ~10 nm diameter nanostructures and that CO transports to Pt adsorption sites by an activated surface diffusion process through the CoO shells surrounding ~2 nm diameter Pt cores. The CO transport process is not due to gas-phase transport below 300 K. The weakly bound adsorbed CO/CoO species responsible for transport was directly observed at ~2147 cm⁻¹ during transport through the CoO shells.

I. Introduction

Recently a Pt@CoO yolk–shell nanostructure, where platinum nanocrystals of several nanometer size are encapsulated in hollow nanostructures of cobalt oxide or cobalt sulfide, was synthesized at the University of California–Berkeley by Yadong Yin et al.¹ It was reported that the Pt@CoO yolk–shell exhibits catalytic activity for the ethylene hydrogenation reaction. Since the catalytic activity of platinum is much higher than that of cobalt or cobalt oxide in this reaction, the reactants and products were postulated to diffuse in and out through the CoO shells to reach the platinum core. This phenomenon was explained by the postulate that small molecules can penetrate through grain boundaries in the polycrystalline CoO shells to reach the internal Pt surface. The observation of the catalytic reaction is not completely definitive for the diffusion process to the interior of Pt@CoO nanostructures, since traces of surface Pt deposited on the outside of the CoO shell or within pores in the CoO shell could also cause ethylene hydrogenation. Electron microscopy indicated that most of the Pt is encased by the CoO shell, but this measurement is not able to definitively detect atomic-size deposits of Pt deposited elsewhere.

An infrared spectroscopic technique, developed previously in the Pittsburgh laboratory for studies of organic molecule diffusion through the pore structure of high-area oxide powders, samples surface diffusion over a macroscopic length scale (~10⁵ nm).² We have applied this same technique to monitor the diffusion of the CO molecule through the ~5 nm thick shells of CoO, observing the arrival of the CO molecules at the internal Pt surface. The measurements are sufficiently sensitive to detect

the weakly adsorbed CO molecules diffusing over CoO sites, indicating that the CO transport through the CoO shell is via a weakly bound CO molecule rather than by a gas-phase process through the internal pore structure of the shell. Thus, in this investigation the infrared spectroscopic method for the direct observation of molecular diffusion through high-area material has been extended downward in length scale by ~4 orders of magnitude.

II. Experimental Methods

The experimental methods to measure the molecular diffusion in this work are described in detail in ref 2. A nanocrystalline powder is pressed into a tungsten grid (0.002 in. thickness) using a hydraulic press.^{3,4} The grid is tightly stretched and clamped into Ni cooling bars which are bolted onto Cu electrical leads originating from a reentrant Dewar, which serves as a manipulator. A type-K thermocouple is welded to the top of the tungsten grid.^{5,6} The temperature as measured by the thermocouple is achieved by resistive heating via the Cu leads using an electronic temperature control program, which heats the sample at a rate of 0.6 K s⁻¹. The sample temperature can be controlled in the range of 83–1500 K when liquid nitrogen (*l*-N₂) is used as a refrigerant with a resolution of 0.1 K in these experiments.

The manipulator which holds the powdered sample on the grid is movable up and down allowing the measurement of the spectrum of two samples supported one above the other together on the grid. This arrangement allows the properties of CoO shells and Pt@CoO samples to be directly compared under exactly the same experimental conditions.

The synthetic production of these CoO and Pt@CoO nanocrystals is described in ref 1. After preparation, the average diameters of the outer CoO shell and the inner Pt yolk in the Pt@CoO nanocrystal were confirmed by transmission electron microscopy (TEM) to be 8–12 nm and 2–3 nm, respectively.

[†] University of Pittsburgh.

[‡] University of California, Riverside.

[§] University of California, Berkeley.

- (1) Yin, Y.; Rioux, R. M.; Endonmez, C. K.; Hughes, S.; Somorjai, G. A.; Alivisatos, A. P. *Science* **2004**, *304*, 711.
- (2) Kim, S.; Byl, O.; Liu, J.-C.; Johnson, J. K.; Yates, J. T., Jr. *J. Phys. Chem. B* **2006**, *110*, 9204.

(3) Ballinger, T. H.; Wong, J. C. S.; Yates, J. T., Jr. *Langmuir* **1992**, *8*, 1676.

(4) Ballinger, T. H.; Yates, J. T., Jr. *Langmuir* **1991**, *7*, 3041.

(5) Basu, P.; Ballinger, T. H.; Yates, J. T., Jr. *Rev. Sci. Instrum.* **1988**, *59*, 1321.

(6) Yates, J. T., Jr. *Experimental Innovations in Surface Science*; Springer-Verlag New York, Inc.: New York, 1998.

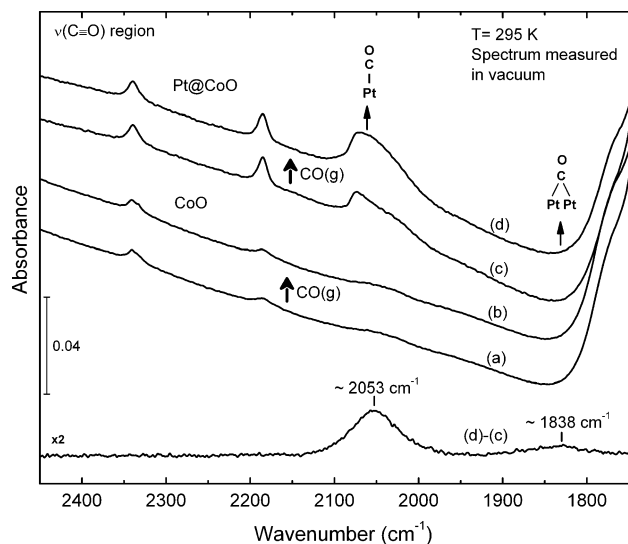


Figure 1. FTIR spectra for CO adsorption (~ 100 torr) in the $\nu(\text{C}=\text{O})$ region at 295 K on CoO (a) before adsorption and (b) after adsorption, followed by evacuation, and on Pt@CoO (c) before adsorption and (d) after adsorption, followed by evacuation.

Gases are introduced into the IR cell through a gas line in which a Baratron capacitance manometer (0–100 torr) is used for pressure measurement. The base pressure as measured by a Bayard–Alpert type ionization gauge is $\sim 1.0 \times 10^{-8}$ torr. To eliminate possible impurity effects from traces of metal carbonyls, the CO storage bulb is immersed in $l\text{-N}_2$ when gas is withdrawn.

The infrared spectra are recorded with a Bruker TENSOR 27 FTIR spectrometer, using a $l\text{-N}_2$ cooled MCT detector. Noise levels in the baseline of the acquired spectra are in the 3×10^{-4} absorbance range. The spectrometer and the enclosed IR cell are purged continuously by dry air from which CO_2 and H_2O have been removed. Each spectrum is obtained by averaging 1024 interferograms at 2 cm^{-1} resolution. The background spectrum taken through the empty grid region is subtracted to eliminate the effect of any gas-phase contribution as well as other small effects in the infrared cell.

III. Results and Discussion

The CoO shells surrounding the Pt cores of the Pt@CoO nanostructures are synthesized from $\text{Co}_2(\text{CO})_8$.¹ As shown in Figure 1, parts a and c, carbonyl stretching modes are observed in the CoO shells without Pt as well as in Pt@CoO in the as-received material. The mode at 2340 cm^{-1} is assigned as CO_2 - (a) and may be due to exposure of each sample to the atmosphere. The vibrational feature at $\sim 2185 \text{ cm}^{-1}$ is assigned as CO bound to the Co^{3+} sites on the CoO shell for both the CoO and Pt@CoO.^{7,8} We note from the literature that during the decarbonylation of $\text{Co}_2(\text{CO})_8$, infrared features in the 2070 and 2030 cm^{-1} region are observed^{9–11} indicating that the CO modes observed in the 2050 cm^{-1} region may be due to subcarbonyl species produced during the decomposition of $\text{Co}_2(\text{CO})_8$ at elevated temperature in the nanostructure synthesis. Upon heating to 600 K, the vibrational features in the 2050 cm^{-1} region disappear, and only the 2185 cm^{-1} feature remains for the material as received (not shown here).

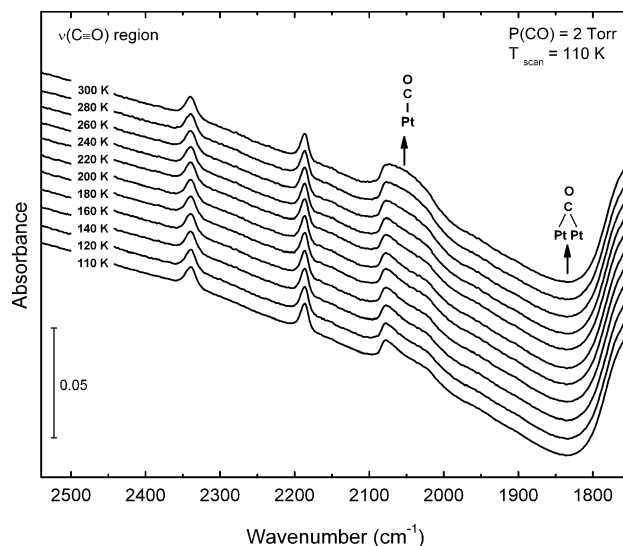


Figure 2. FTIR spectra for CO transport through Pt@CoO at 110 K and after heating the sample (120–300 K). All the spectra were taken at 110 K after cooling the sample, at an equilibrium CO pressure of 2 torr.

Spectra 1b and 1d are observed after treatment of both samples with $\text{CO}(\text{g})$ at 100 torr and 295 K. By obtaining the difference spectrum (d) – (c), the spectral developments due to CO adsorption on Pt@CoO may be observed as shown in the lower portion of Figure 1. Features at ~ 2053 and at $\sim 1838 \text{ cm}^{-1}$ are observed to develop, and these are assigned as the characteristic terminally bound CO and bridge-bound CO on Pt.^{12–14} This experiment therefore shows that at 295 K, CO can transport through the CoO shell to find Pt adsorption sites on the Pt core of the nanostructure. These spectral features do not develop on the CoO shells which do not contain Pt, as seen in spectra a and b of Figure 1. It is noteworthy to point out, as will be shown in detail later, that the CO/Pt modes do not develop at 120 K due to the limited mobility of CO through the CoO shell at this low temperature. This observation indicates that Pt sites are not present on the outer surface of the CoO shells in Pt@CoO, since CO adsorption should occur on such sites at 120 K.

Figure 2 shows the temperature dependence of the spectral developments as Pt@CoO is exposed to $\text{CO}(\text{g})$ at 2 torr. Here, the sample under $\text{CO}(\text{g})$ is programmed upward from 110 K at 0.6 K s^{-1} and cooled back to 110 K for the spectral scan. The subtle changes in the spectra are best seen by difference spectra shown in Figure 3 for Pt@CoO. Here, the temperature dependence of three carbonyl bands at ~ 2147 , ~ 2050 , and $\sim 1836 \text{ cm}^{-1}$ may be observed. The latter two bands indicate the chemisorption of CO on the Pt cores of Pt@CoO.^{12–14} The 2147 cm^{-1} band is due to a weakly bound, mobile adsorbed CO species on the CoO sites surrounding the Pt cores. It becomes visible as CO diffusion into the interior of the CoO shell material occurs. This assignment is confirmed in Figure 4, where the 2147 cm^{-1} band is the only temperature-dependent feature observed for CoO shells without Pt when exposed to $\text{CO}(\text{g})$.

The temperature dependence of the kinetic processes at work in the transport of CO through the CoO shells to the

(7) Busca, G.; Guidetti, R.; Lorenzelli, V. *J. Chem. Soc., Faraday Trans.* **1990**, 86, 989.
 (8) Mergler, Y. J.; Aslst, A. v.; Delft, J. v.; Nieuwenhuys, B. E. *J. Catal.* **1996**, 161, 310.
 (9) Bor, G. *Spectrochim. Acta* **1963**, 19, 1209.
 (10) Kurhinen, M.; Pakkanen, T. A. *Langmuir* **1998**, 14, 6907.
 (11) Suvanto, S.; Pakkanen, T. A.; Backman, L. *Appl. Catal., A: General* **1999**, 177, 25.

(12) Eischens, R. P.; Pliskin, W. A. *Adv. Catal.* **1958**, 10, 1.
 (13) Garland, C. W.; Lord, R. C.; Troiano, P. F. *J. Phys. Chem.* **1965**, 69, 1188.
 (14) Mihut, C.; Descorme, C.; Duprez, D.; Amiridis, M. D. *J. Catal.* **2002**, 212, 125.

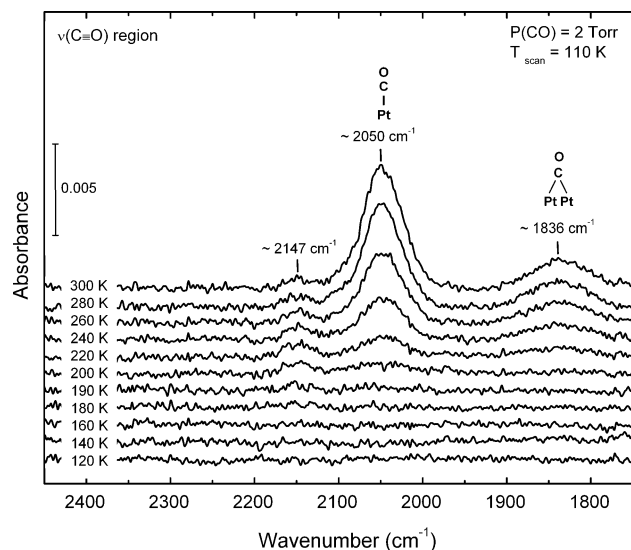


Figure 3. Difference spectra for CO transport through Pt@CoO upon raising the sample temperature (120–300 K), which were obtained by subtracting the initial spectrum at 110 K, which is shown as the lower spectrum in Figure 2.

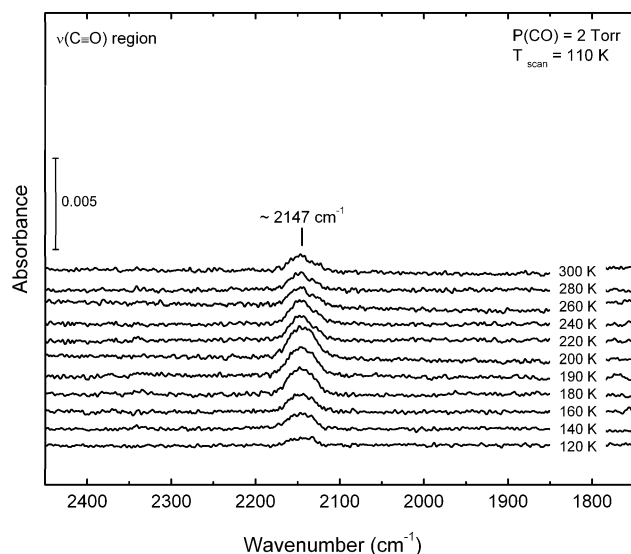


Figure 4. Difference spectra for CO transport through CoO upon raising the sample temperature (120–300 K), which were obtained by subtracting the initial spectrum at 110 K.

internal Pt cores is shown in Figure 5. At $P(\text{CO}) = 2$ torr and at about 160 K, the integrated absorbance of adsorbed CO on CoO sites ($\sim 2147 \text{ cm}^{-1}$) intensifies and maximizes near 215 K. Concomitant with the penetration of adsorbed CO into the CoO shells, Figure 5 shows that the $\sim 2050 \text{ cm}^{-1}$ band due to CO/Pt begins to intensify slightly also near 160 K, but that the rate of intensification becomes much greater above $\sim 215 \text{ K}$, when the CO/CoO band has maximized its intensity. This behavior strongly suggests that weakly bound CO, adsorbed on CoO sites within the shell structure surrounding the Pt clusters in Pt@CoO, kinetically feeds CO to the encapsulated Pt sites.

Figure 6 shows a schematic view of the kinetic processes at work in supplying CO to Pt@CoO nanostructures. We observe the presence of a weakly bound CO/CoO species (at ~ 2147

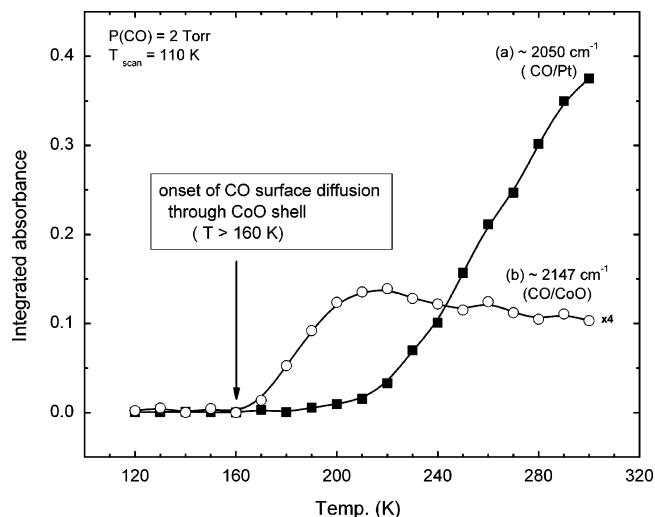


Figure 5. Plot of the integrated absorbance of (a) the terminally bound CO on Pt at $\sim 2050 \text{ cm}^{-1}$ and (b) the weakly bound CO in the CoO shells at $\sim 2147 \text{ cm}^{-1}$ as a function of temperature.

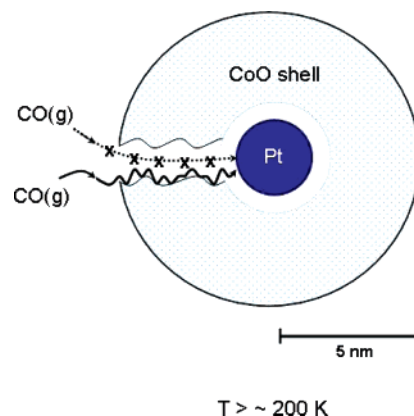


Figure 6. Schematic picture of the CO diffusion through the CoO shells in Pt@CoO.

cm^{-1}) which are populated prior to arrival of CO molecules at the encapsulated Pt sites; these weakly bound species mediate the transport of CO into the interior of the Pt@CoO nanostructures. In Figure 6, we schematically indicate that transport of CO(g) through the CoO shell walls does not supply CO to the internal Pt sites. The lack of such gas-phase transport (Knudsen transport) through the pore structure of the CoO shells is confirmed by the absence of evidence for CO/Pt species when the temperature is below $\sim 200 \text{ K}$.

These results have implications in the use of encapsulated metal nanostructures for heterogeneous catalysis. Such nanostructures may well have antisintering properties which plague many conventional supported metal catalysts. However, using the Pt@CoO structures as an example, at lower temperatures in such catalysts it may be necessary to consider only adsorbed phases within the shell structure as the transport media for reactants and products moving to and fro to the internal catalytic site. More favorable rate processes involving gas-phase transport may be lacking or limited. As the temperature of such nanostructure catalysts is raised, the sticking coefficient for the transporting phases within the pore structure of the shell will decrease and the rate of material transport may then reach that of gas-phase transport through the pores.

IV. Summary

The molecular transport of adsorbed CO molecules through the CoO shells in Pt@CoO nanostructures was observed using transmission FTIR spectroscopy, probing the development of characteristic IR modes of the adsorbed CO species on the Pt yolk. In addition, the FTIR observation of weakly bound CO within the pore structure of the CoO shells indicates that the

transport of CO occurs by the surface diffusion of the weakly adsorbed molecule below 300 K. The onset of the CO diffusion through the CoO shells in Pt@CoO occurs at ~ 160 K.

Acknowledgment. We acknowledge with thanks the support of the Department of Energy, Office of Basic Energy Sciences.

JA072588G